Atmospheric Free Modes and Subtropical High*

TAO Li (陶 丽) and LU Weisong(陆维松)

Nanjing University of Information Science and Technology, Nanjing 210044

(Received January 7, 2004; revised August 31, 2004)

ABSTRACT

By numerically solving the unforced and inviscid nonlinear barotropic vorticity equation through the quasi-Newton method, the steady free modes are obtained, which are very similar to the real flow fields, and their scatter diagram of (ψ, q) display segmented linear or nonlinear relations. From this scheme a range of free modes have been achieved, each corresponding to one of the atmospheric flow fields. In the study of changes in the western Pacific subtropical high (WPSH) as revealed by free modes it is discovered that the west-extension/northward jump and east-movement/southward withdrawal of WPSH for the free mode occur 5-10 days ahead of the changes in the high as shown in the 500 hPa geopotential height field. Besides, a standard mode technique is adopted to investigate the stability of the free modes, indicating that the faster the instable mode grows, the closer it comes to a quasi-steady state. Especially, the instable mode with its quasi-steady state growing the fastest bears a correspondence with the high in steady intensification, leading to the fact that the persistent strengthening of the high is likely to be caused by the instable free modes with the fastest growth that are of quasi-steady state, or experience long-period low-frequency variation.

Key words: free mode, western-Pacific subtropical high, instability

1. Introduction

Subtropical highs are the warm systems over bihemispheric subtropics, exerting great effect on the occurrence of the rainy reason, flood-drought, heavy rain, etc. in China through the changes in position and intensity. In recent years, in particular, the persistent anomaly of the high has resulted in frequent happening of severe meteorological disasters, so that it has become one of the leading topics of atmospheric sciences. Over the past decades scientists have made a lot of efforts to uncover the laws of the high's activities, especially those in the western Pacific. Tao et al. (1963) and Huang (1979) achieved striking results by a diagnostic technique. Wu et al. (2002) derived many important findings in their comprehensive in-depth research of the high's formation and variation. In early stages the low-order spectral method obtained multi-equilibrium states were often utilized for the high's northward displacement and subsequently, Fan and Miao (1996) explained the genesis by means of Rossby soliton theory. However, subtropical highs differ in formation more greatly from blocking highs, and particularly the meridional shift of the high is just a change in position, with few or no change for the related flow pattern, which differs greatly from the multiple equilibria of different spase flow patterns associated with meridional and zonal circulations of high- and low-index at extratropics. Therefore, it seems difficult to expound the variation of the subtropical high by use of the multi-equilibrium theory. In contrast, the soliton is an idealized solution of free mode derived analytically from a simplified theoretical model rather than directly from real data, so that the result differs to greater extent from observational fact. Branstator and Opsteegh (1984) used observations to investigate free modes in studying atmospheric motion, thereby overcoming the limitations for the inconsistency of a soliton solution with the facts of the real atmosphere. So far, no reports have been published regarding the application of general free modes to the study of subtropical highs. Under the equilibrium of diabatic heating with friction a subtropical high can be regarded as a single quasi-steady free mode solution of the quasi-geostrophic and nonlinear barotropic vorticity equation that is numerically approximated by observations as the initial iterative fields. Obviously, the quasi-steady free mode comes from the stepwise

*The work is supported by the National Natural Science Foundation of China under Grant No. 40275016.

adjustment of the data field, leading to more similarity of the mode high-related flow pattern to that of the actual high. For longer-term statistical mean, diabatic heating is balanced by friction, such that the free mode is able to describe a longer-term variation in the high. To be closer to the real atmospheric condition the work first presents the subtropical high's formation and variation by means of the general free modes in an attempt to determine the free mode growing the fastest by which to detect the precursor for the high's variation.

2. Principle and data

2.1 *Principle for finding the free mode*

Starting from the spherical non-divergent nonlinear barotropic vorticity equation, we now determine a free mode. For simplification we take into account only a steady free mode to establish a direct relationship between observations and the solution to be found. Hence, we shall seek the solution of the following dimensionless steady barotropic vorticity equation

$$J(\psi, \bigtriangledown^2\psi + f) = 0, \tag{1}$$

where ψ is the stream function, f the Coriolis parameter and $J(A,B) = \dfrac{1}{\cos\phi}\Big(\dfrac{\partial A}{\partial\lambda}\dfrac{\partial B}{\partial\phi} - \dfrac{\partial B}{\partial\lambda}\dfrac{\partial A}{\partial\phi}\Big)$. $(2\Omega)^{-1}$ is set to be the time scale in which Ω denotes the angular velocity of earth's rotation. To solve the field of stream function ψ satisfying Eq.(1), we define a functional of the form

$$F(\psi) = \frac{1}{4\pi}\int_{-\frac{\pi}{2}}^{\frac{\pi}{2}}\int_{0}^{2\pi}[J(\psi, \bigtriangledown^2\psi + f)]^2\cos\varphi \mathrm{d}\varphi\mathrm{d}\lambda, \tag{2}$$

which represents the deviation of a given flow field from the steady free conditions. Finding a free mode is changed to acquiring the minimal value of F and determining whether F is close to zero. Here, ψ is denoted by a spherical harmonic function with the parallelogram truncation at wavenumber 15, followed by seeking the extremum of Eq.(2) by the quasi-Newton method. However, before the use of this method it is necessary to get the first-order derivative of F with respect to ψ as shown below

$$\frac{\partial F}{\partial\psi} = 2\Big\{\ \bigtriangledown^2\ J[J(\psi,q),\psi] - J[J(\psi,q),q]\Big\}, \tag{3}$$

where $q = \bigtriangledown^2\psi + f$ is the absolute vorticity. To get a solution similar to the one of the real atmosphere we make use of the flow field of actual observations as the initial field for iteration by the quasi-Newton method. Moreover, the Eq.(2)-given free mode's amplitude, being smaller compared to the one in the actual flow field, should be corrected by adding the deviation to the study flow field $\widetilde{\psi}$, leading to a new functional of the form

$$\begin{aligned} F(\psi) &= \frac{1}{4\pi}\int_{-\frac{\pi}{2}}^{\frac{\pi}{2}}\int_{0}^{2\pi}\Big\{[J(\psi, \bigtriangledown^2\psi + f)]^2 \\ &\quad +\mu(\psi - \widetilde{\psi})^2\Big\}\cos\varphi \mathrm{d}\varphi\mathrm{d}\lambda, \end{aligned} \tag{4}$$

in which $\widetilde{\psi}$ denotes the actual flow field and μ takes, in order, dimensionless values of 1, 0.01, 0.0001, and 0, and the related iterative initial field is composed of $\widetilde{\psi}$ and the free solution from a preceding μ. Consequently, because of μ= 0 in the end, the solution of Eq.(4) for the minimum should be a free solution that is the closest to the actual flow field. Similarly, the first-order derivative of F with respect to ψ has the form

$$\begin{aligned} \frac{\partial F}{\partial\psi} &= 2\Big\{\ \bigtriangledown^2\ J[J(\psi,q),\psi] - J[J(\psi,q),q]\Big\} \\ &\quad +2\mu(\psi - \widetilde{\psi}). \end{aligned} \tag{5}$$

This work utilized 500 hPa winds from May 26 to August 8, 1998 with which to get a real flow field, followed by using the day-to-day actual fields as the initial fields to find the solutions to the minimal values of Eq.(4) through the iteration by the quasi-Newton method, resulting in a group of free modes, of which the stability is examined by the standard mode to reveal instable free modes.

2.2 *Stability of free modes*

Assume a steady free mode to be subject to a perturbation, leading to

$$\psi = \psi_0 + \psi', q = q_0 + q', \tag{6}$$

in which $q_0 = \nabla^2\psi_0 + f$ and $q' = \nabla^2\psi'$. Setting ψ_0 to be a steady free solution and ψ' to be a perturbation,

we get the spherical barotropic non-divergent vorticity equation

$$\frac{\partial q}{\partial t} + J(\psi, q) = 0, \tag{7}$$

which is rewritten as

$$\frac{\partial q'}{\partial t} + J(\psi_0, q') + J(\psi', q_0) + J(\psi', q') = 0, \tag{8}$$

and linearizing Eq.(8) leads to

$$\frac{\partial q'}{\partial t} + J(\psi_0, q') + J(\psi', q_0) = 0. \tag{9}$$

Assume the perturbation to be denoted by the standard mode:

$$\psi'(\lambda, \phi, t) = \mathrm{Re}\lfloor \xi(\lambda, \phi) \mathrm{e}^{\nu t} \rfloor, \tag{10a}$$

$$q'(\lambda, \phi, t) = \mathrm{Re}\lfloor p(\lambda, \phi) \mathrm{e}^{\nu t} \rfloor, \tag{10b}$$

where ν, ξ and p are normally complex numbers, i.e., $\nu = \nu_r + \mathrm{i}\nu_i, \xi = \xi_r + \mathrm{i}\xi_i$, and $p = p_r + \mathrm{i}p_i$, in which ν_r, ξ_r, and $p_r(\nu_i$, ξ_i, and $p_i)$ are the corresponding real (imaginary) parts. According to the relation between q' and ψ', we have

$$p = \nabla^2 \xi. \tag{11}$$

If ν_r is a positive (negative or zero) value the factor $\exp(\nu_r t)$ in the brackets of Eq.(10a, b) increases temporally with exponential growing (decaying or constant) and has an e-folding time of $\tau \equiv \mid 1/\nu_r \mid$. The other bracketed terms display periodic variations at periods $T = \mid 2\pi/\upsilon_i \mid$.

Putting Eq.(10) into Eq.(9) results in

$$\nu p + J(\psi_0, p) + J(\xi, q_0) = 0, \tag{12}$$

which is an eigenvalue equation, where ν is the eigenvalue and p the eigenvector (with corresponding ξ given). Denote an eigenvalue as $\nu^m = \nu_r^m + \mathrm{i}\nu_i^m$ and its eigenvectors $\xi^m = \xi_r^m + \mathrm{i}\xi_i^m$ and $p^m = p_r^m + \mathrm{i}p_i^m$ and as soon as one of the ν_r^m is positive, the steady free mode $\psi_0(q_0)$ is instable; and when all ν_r^m are negative or zero the mode is stable. To get the cases of ν_r^m, the spectral method is used to numerically solve the eigenvalue Eq.(12) [see Verkley, 1987].

2.3 *Data source diagnosis and analysis*

The data used are global daily mean NCEP-/NCAR reanalysis data at resolution of 2.5° × 2.5°lat./long. from May 26 to August 8, 1998.

3. Diagnosis and analysis

3.1 *Features of the free mode*

The obtained free mode refers to the solution to $J(\psi, q) = 0$. Here $q = \nabla^2\psi + f$ is absolute vorticity, suggesting that $\psi = \psi(q)$ and points in the scatter diagrams of (ψ, q) should be arranged in a curve or a straight line rather than in a divergent form. Figures 1a and 1b are the scatter diagrams of actual (ψ, q) and free mode $(\psi_\mathrm{E}, q_\mathrm{E})$, respectively, on June 17, 1998 with Fig.1a (1b) related $F_1 \approx 4.055 \times 10^{-4} (F_2 \approx 6.428 \times 10^{-8})$ in dimensionless form, leading to $F_2/F_1 \approx 10^{-4}$, which shows that F_2 is small enough compared to F_1 as the iterative initial field, whose ψ is viewed as a steady free mode. It is obvious that the F_2–related point distribution (Fig.1b) is greatly narrowed compared to F_1 (Fig.1a). Figure

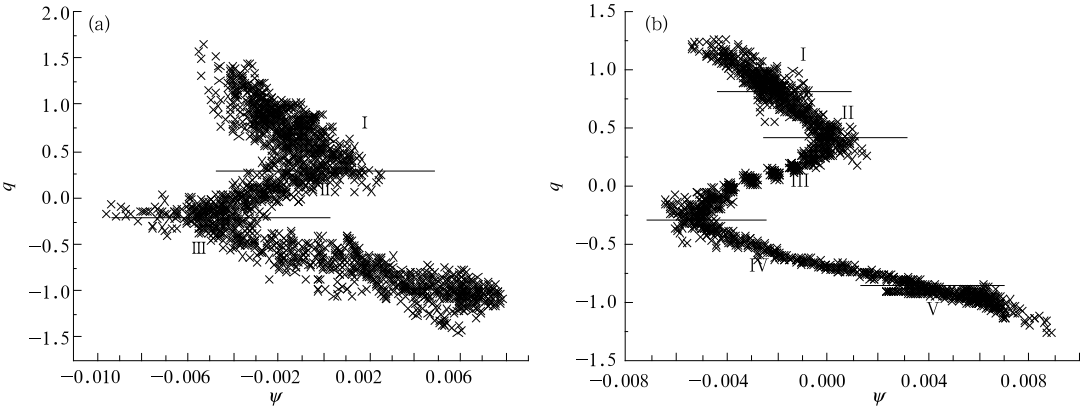

Fig.1. Scatter diagrams of (ψ, q) for the actual flow field (a) and the free mode flow field (b) on June 17, 1998.

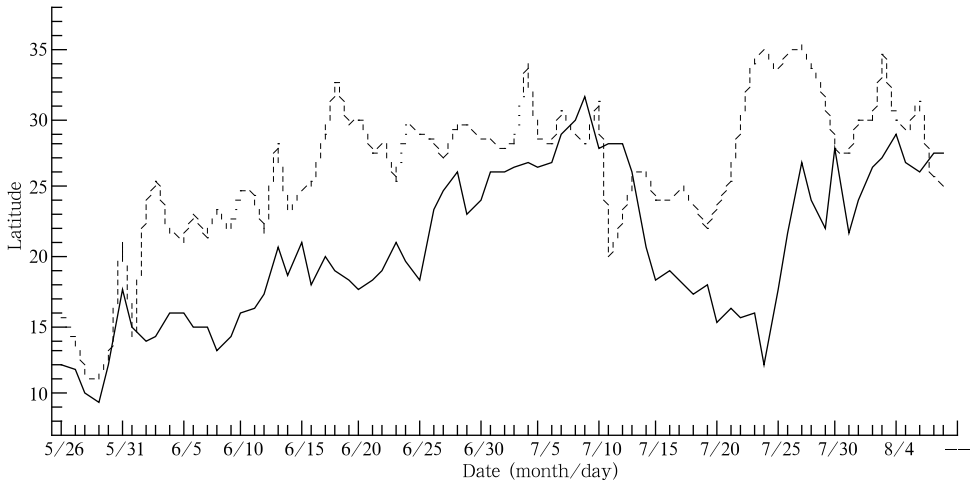

Fig.2. Daily variation in position of the ridge line for the subtropical high from the mean over 110°-130°E (solid line) vs the free mode-given results (dotted line) for the summer of 1998.

1b depicts 5 zones of the scatter diagram based on (ψ, q) from different functions and point divergence, of which zones I and V refer to free modes ψ_{E} at bihemispheric high latitudes on June 17 (see also Fig.2 for the free mode variation in part of the globe), and zones II and IV (III) refer to subtropical (equatorial) latitudes on both hemispheres. Analysis of (ψ, q) scatter points in Fig.1b shows segmented linear or nonlinear relations, a pattern that differs greatly from well-known forms of free mode-type R-H (Rossby-Haurwitz) wave, dipole and soliton in that on the scatter diagram the R-H wave (dipole) is displayed as a straight line (crossed lines).

3.2 *Variation of the free mode subtropical high in the summer of 1998*

Persistent severe precipitation occurred in June - August of 1998 over the Middle and Lower Reaches of the Yangtze River, creating an exceptionally big flood on a 100-yr return basis since 1954 that did unprecedented damage to national economy and tremendous loss of lives and properties. The event bore a relation to the northward movement and maintenance of the western-Pacific subtropical high, and the occurrence of the second Meiyu season during the high's southward withdrawal. In the early and mid decades of June the 120°E ridge line (averaged over 110°-130°E) shifted from 15°N slowly northward, reaching 17°N on June 12 and maintaining dominantly in 17°-21°N during June 12-28 for the first Meiyu season. The ridge made a apparent jump northward on 25 June, arriving at 26°N on June 28, the first Meiyu ended and put the Middle and Lower Reaches of the Yangtze River under the control of the subtropical high with little or no rain falling there from June 29 to July 20. The ridge reached the northernmost limit of 32°N on June 9 and subsequently it began to retreat south at rapidity, arriving at 16°N on July 21 during which a so-called "second Meiyu season" began south of the River, resulting in floods over the basin, and in that period the ridge started its northerly jump from 12°N on July 24 to 28°N on July 30, 1998 with the second Meifu season ended on July 31.

Figure 2 depicts the variation of the free mode subtropical high ridge at 120°E averaged over 110°-130°E (dotted line) vs the observed high's daily shift in position (solid line) in June-August, 1998, indicating that the free mode-given high shows its first northerly jump from the end of May to the beginning of June, with the ridge reaching the vicinity of 24°N on June 2 and maintaining between 21°-25°N in during June 2-16, and the ridge exhibited its apparent jump northward on June 17, arriving at around 33°N the next day. The fact shows that the first Meiyu season began on June 2 and ended on 16 of the month. Now look at the free modes, which indicate that the high's second

northerly jump happened on July 4, when the ridge arrived at its northernmost limit of 34°N and afterwards it began to withdraw southward and swung between 20° to 26°N during July 11-19, ushering in the second Meiyu rainfall process. And the ridge began its big jump northward from 22°N on July 19, reaching about 35°N on July 27, indicative of the ending of the second Meiyu season.

To sum up, the subtropical high for the free mode shows its first and second northerly shifts to be 10 days ahead of the observed, its big southerly withdrawal to be 5 days in advance and southerly shift/northerly jump to be 5 days ahead as well compared to the actual high. It follows that the free mode high starts its northerly and southerly movement about 5-10 days earlier than the atmospheric counterpart.

We can further understand the in-advance movement of the free mode high in its journey from Fig.3 in 0-60°N, 60°E-120°W, which depicts the 500 hPa height fields (denoted as I), the actual flow fields, i.e., the initial iterative fields (as II) and free modes (as III) for each of four sets. From each initial iterative field (II) we get a free mode (III), the latter being close but not identical to the former. From Fig.3a we see that I-given 588 dagpm line moves north of the Taiwan of China around 25°N and extends westward as far as 100°E on June 13, with the Jiang-Huai Meiyu rainfall happening; Fig.3a-II shows that the observed high of June 2 is south- and eastward of that in Fig.3a-I on June 13 but the free mode high of Fig.3a-III shifts northward and extends westward, resulting in a high's core in the south of China mainland. In Fig.3b-I the high makes further northerly displacement, extending west to 90°E, with the end of the first Jiang-Huai Meiyu season; the Fig.3b-II high is more south- and eastward of mean on June 18, which indicates that the rainband remains in Middle and Lower Reaches of the Yangtze River, and in contrast, on the day the free

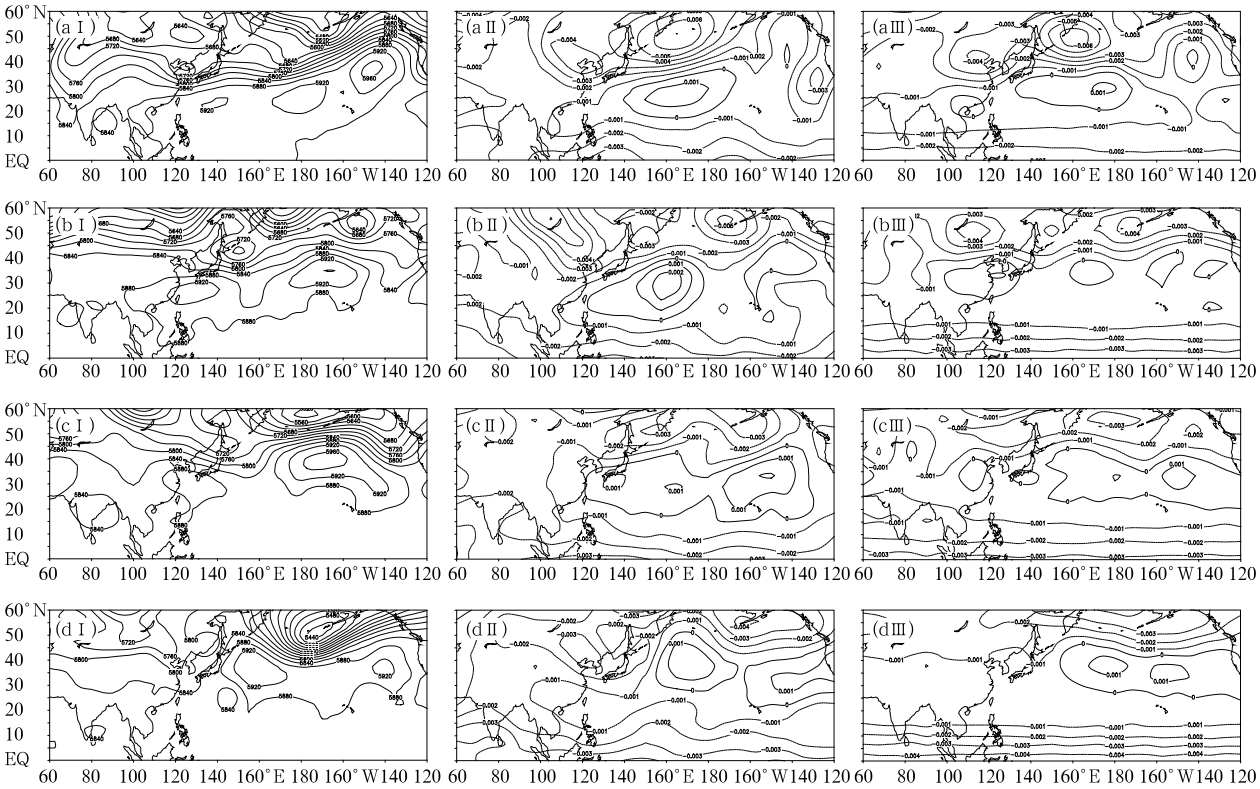

Fig.3. The 500-hPa height field on June 13, June 28, July 9 and July 24, respectively, in the left panel (I) of 3a, 3b, 3c and 3d; the actual flow field on June 2, June 18, July 4 and July 19, respectively, in the middle panel (II) of 3a, 3b, 3c and 3d, with related free mode given in the right panel (III).

mode high moves further northwest, controlling the east of the mainland, suggestive of the end of the rainy season over the Yangtze Basin. The high of Fig.3c-I moves to its northernmost limit on July 9 in company with an anticyclone in North China; the free mode high shifts to its northernmost limit on July 4, with a center in NE China, a situation quite analogous to that of the height field (Fig.3c-I) on July 9. We see that on July 24 the Fig.3d-I 588 dagpm line has left the mainland; on July 19 the Fig.3d-II anticyclone stretches west to the central-eastern mainland while the free mode high's main body is located over the North Pacific.

From the foregoing analysis we see that the westerly extension and northerly shift of the free mode high begin earlier than those of the actual high and so do the southward withdrawal and eastward shift, thereby indicating that in addition to external factors, the internal synoptic dynamic factors have noticeable effects on the variation of the subtropical high.

3.3 *Analysis of the stability of free modes*

By calculating the eigenvalue equation of free modes, we get corresponding eigenvalues and eigenvectors. The free modes have a lot of positive ν_r^m, thus showing that they are (may be) barotropicly instable, i.e., the amplitude of a small perturbation on the basic flows would increase and the distribution of their eigenvalues is analogous to that of Fig.4, i.e., distributed along the axes of $\nu_i = 0$ and $\nu_r = 0$. The first case suggests that points of $\nu_r \neq 0$ are mainly distributed along the $\nu_i = 0$ axis, implying that the instable modes are quasi-steady, or undergoing low-frequency variation, and points of greater $\mid \nu_r \mid$ tend more intensely to be distributed along the $\nu_i = 0$ axis, meaning that the free modes have stronger instability, approaching more intensely a quasi-steady state, and, particularly the modes growing fastest approach the state more readily, indicating their very intense locality. And the second case is concerned with points distributed along the $\nu_r = 0$ axis, suggesting that points of $\nu_i \neq 0$ are dominantly distributed along the $\nu_i = 0$ axis, meaning that stable are non-steady modes and especially those displaying high-frequency variation and the points of bigger $\mid \nu_i \mid$ tend more strongly to be along the $\nu_r = 0$ axis, implying that the shorter the period of free modes, the closer to a stable state they are, indicating their slow growth. Of the free modes obtained here, the ones growing fastest have their e-folding times τ ranging over 18.1 and 6.1 days, both with periods T more than 22 days, which means that the fastest growing modes are quasi-steady, or exhibiting low-frequency variation, and they grow fastest at fixed positions. Such modes have strong locality so that, although a range of free modes growing fastest is available, only those in the neighborhood of the western Pacific are related to the intensification of the subtropical high of western Pacific's origin. As depicted in Fig.5, the fastest growing modes of June 8, 1998 correspond to the wave train in the North Pacific running along 30°N from west to northeast, with its positive- (negative-) value center in the western (middle) part of the ocean and a positive core from the Okhotsk to the Bering Sea, which is the fastest growing wave packet produced by barotropic instability, ushering in the reinforcement of the subtropical high in this region. The subtropical high is steadily reinforced in the first decade of June and its 120°E ridge (mean over 110°-130°E) moves northward slowly from 15°N, reaching 17°N on June 12, and thereby producing Meiyu rainfall during June 12-28. This indicates that the persistent intensification of the high is likely to be caused by the fastest growing modes that are quasi-steady, or undergoing low-frequency variations.

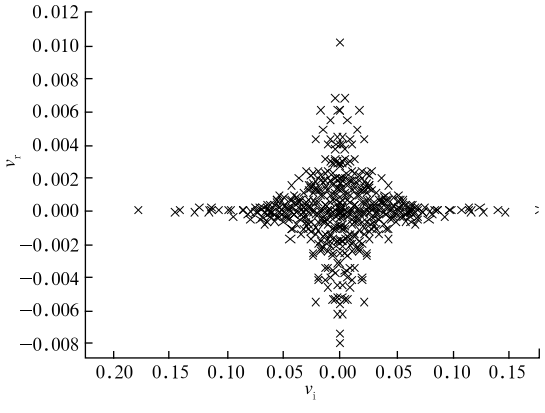

Fig.4. Plot of eigenvalues of free modes for June 7, 1998, with the ordinate (abscissa) denoting the real (imaginary) part of the mode.

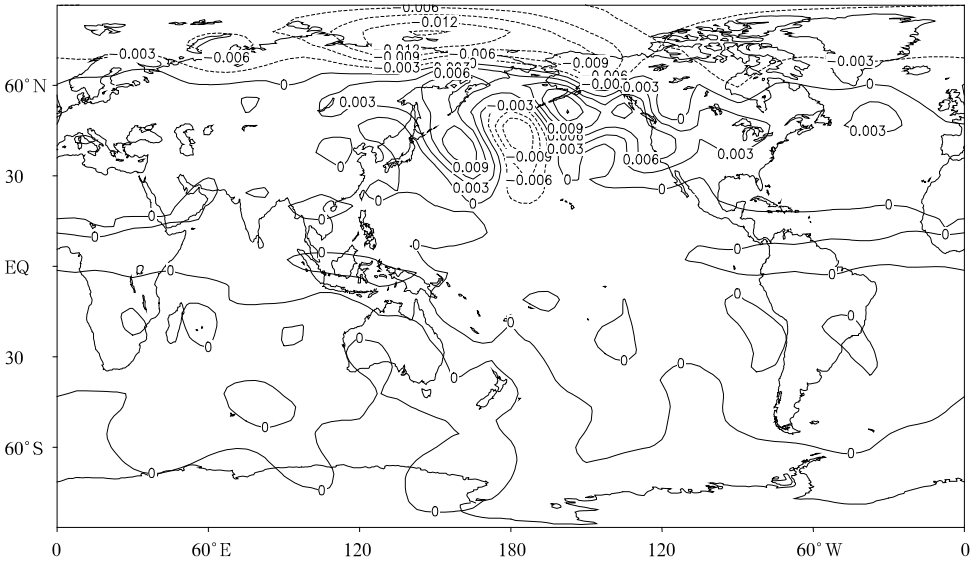

Fig.5. Distribution of fastest growing free modes on June 8, 1998.

4. Discussion and results

Preliminary studies of free modes have been undertaken only abroad, but they are limited to very few examples of free modes, and on the importance of free modes to weather/climate and concerning their correspondence to actual synoptic processes no papers have been published at home and abroad. The present work makes the first attempt to investigate the evolution of the western Pacific subtropical high associated with the 1998 exceptionally severe rainstorm in China, for which the quasi-Newton iteration is employed to solve the non-forcing, non-dissipative nonlinear barotropic vorticity equation, resulting in daily free modes similar to the actual flow fields from May 26 to August 8, and in terms of the free modes analysis is undertaken of the mechanism of changes in the high. Examination of the actual flow fields and free modes shows that the free mode high has its westerly extension, northerly jump, easterly shift and southerly withdrawal earlier 3−11 days compared to the actual high, revealing the dynamic mechanism for the high's development, by which the great effects of the atmospheric internal dynamic factors upon the development are illustrated.

The free modes obtained by the variational scheme in this work may be subject to barotropic instability and the faster growing modes exhibit more quasi-steadiness, showing strong locality. In particular, the instable modes with the fastest growing quasi-steady state are related to the steadily enhanced high and the enhancement may be caused by the fastest growing unstable free modes that are quasi-steady, or experiencing low-frequency variation.

REFERENCES

Anderson, J. L., 1991: The robustness of barot ropic unstable modes in a zonally varying atmosphere. *J. Atmos. Sci.*, **48**, 2393-2410.

Baines, P. G., 1976: The stability of planetary wave on sphere. *J. Fluid Mech.*, **73**, 193-213.

Fan Hong and Miao Jinhai, 1996: Rossby soliton theory on the formation of subtropical and blocking highs. II. The critical layer. *Acta Meteorologica Sinica*, **54**(6), 722-729. (in Chinese)

Grant Branstrator, and J. D. Opsteegh, 1989: Free soliton of the barotropic vorticity equation. *J. Atmos. Sci.*, **46**, 1799-1814.

Hoskins, B. J., 1973: Stability of the Rossby-Haurwitz wave. *Quart. J. Roy. Meteor. Soc.*, **99**, 723-745.

Huang Shisong, 1979: Study of western Pacific subtropical highs. *Meteorological Monthly*, **5**(10), 1-3. (in Chinese)

Leith, C. E., 1983: *Predictability in theory and practice in Large-Scale Dynamic Processes in the Atmosphere.* Academic Press, 365 pp.

Lorenz, E. N., 1972: Barotropic instability of Rossby wave motion. *J. Atmos. Sci.*, **29**, 258-264.

Simmons, A. J., J. M. Wallace, and G. B. Branstator, 1983: Barotropic wave propagation and instability, and atmospheric teleconnection patterns. *J. Atmos. Sci.*, **40**, 1363-1392.

Tao Shiyan, Zhu Fukang, and Wu Tianqi, 1963: *Synoptic study on subtropical high's activities over China mainland and its neighboring seas in summer*, In: Study on Some problems of Summer Subtropical Weather Systems over China. China Scientific Press, Beijing, pp.106-123. (in Chinese)

Verkley, W. T. M., 1987: Stationary barotropic modons in westerly background flow. *J. Atmos. Sci.*, **44**, 2383-2398.

Wu Guoxiong, Chou Jifan, Liu Yimin, and He Jinhai, 2002: *Dynamic aspects of the formation and variation of subtropical highs*. Science Press, Beijing. (in Chinese)